Quantum Dot Light-Emitting Transistors-Powerful Research Tools and Their Future Applications

Kahmann, Simon; Shulga, Artem; Loi, Maria A.

Published in:
Advanced Functional Materials

DOI:
10.1002/adfm.201904174

Publication date:
2020

Creating Flavin Reductase Variants with Thermostable and Solvent-Tolerant Properties by Rational-Design Engineering

Somchart Maenpuen,[a] Vinutsada Pongsupasa,[b] Wiranee Pensook,[a] Piyanuch Anuwan,[b] Napatsorn Kraivisitkul,[c] Chatchadaporn Pinthong,[d] Jittima Phonbuppha,[b] Thikumporn Luanloet,[e] Hein J. Wijma,[f] Marco W. Fraaije,[f] Narin Lawan,[g] Pimchai Chaiyen,[b, e] and Thanyaporn Wongnate*[b]

We have employed computational approaches—FireProt and FRESCO—to predict thermostable variants of the reductase component (C_1) of (4-hydroxyphenyl)acetate 3-hydroxylase. With the additional aid of experimental results, two C_1 variants, A166L and A58P, were identified as thermotolerant enzymes, with thermostability improvements of 2.6–5.6 °C and increased catalytic efficiency of 2- to 3.5-fold. After heat treatment at 45 °C, both of the thermostable C_1 variants remain active and generate reduced flavin mononucleotide ($FMNH^-$) for reactions catalyzed by bacterial luciferase and by the monooxygenase C_2 more efficiently than the wild type (WT). In addition to thermotolerance, the A166L and A58P variants also exhibited solvent tolerance. Molecular dynamics (MD) simulations (6 ns) at 300–500 K indicated that mutation of A166 to L and of A58 to P resulted in structural changes with increased stabilization of hydrophobic interactions, and thus in improved thermostability. Our findings demonstrated that improvements in the thermostability of C_1 enzyme can lead to broad-spectrum uses of C_1 as a redox biocatalyst for future industrial applications.

Introduction

Enzymes play a major role in biotechnology and serve as attractive, efficient, selective, and sustainable biocatalysts for processes involved in the production of pharmaceuticals, fine chemicals, and biofuels.[1,2] However, the issue of protein instability poses a fundamental challenge to the use of enzymes for practical-scale syntheses and chemical manufacturing, because these often require harsh reaction conditions such as elevated temperatures and exposure to organic solvents.[1] Because of these limitations, stabilization of proteins against thermal and chemical denaturation has been a longstanding goal in enzyme engineering. As well as providing improved robustness under harsh operational conditions, increasing the thermostability of a protein can also enhance its evolvability for various applications.[3]

A variety of methods, including immobilization,[4,5] medium engineering,[6] and protein engineering,[7] have been used to improve the thermodynamic and kinetic stability of enzymes. In protein engineering, directed evolution and semirational or rational design are three general methods employed to obtain thermostable variants of a target enzyme.[6] A number of studies have shown that directed evolution can enhance the performance of enzymes at elevated temperatures.[8,9] However, this technique requires screening of large numbers of clones (e.g. >10000); this is laborious and time-consuming and typically requires several rounds of mutagenesis and screening to

[a] Asst. Prof. Dr. S. Maenpuen, W. Pensook
Department of Biochemistry, Faculty of Science, Burapha University
169 Long-Hard Bangsaen Road, Chonburi, 20131 (Thailand)

[b] V. Pongsupasa, P. Anuwan, J. Phonbuppha, Prof. Dr. P. Chaiyen, Dr. T. Wongnate
School of Biomolecular Science and Engineering
Vidyasirimedhi Institute of Science and Technology (VISTEC)
555 Moo 1 Payupnai, Wangchan, Rayong, 21210 (Thailand)
E-mail: thanyaporn.w@vistec.ac.th

[c] N. Kraivisitkul
Kamnoetvidya Science Academy
999 Moo 1 Payupnai, Wangchan, Rayong, 21210 (Thailand)

[d] Dr. C. Pinthong
Department of Chemistry, Faculty of Science
Srinakharinwirot University
114 Sukhumvit 23 Road, Bangkok, 10110 (Thailand)

[e] T. Luanloet, Prof. Dr. P. Chaiyen
Center for Excellence in Protein and Enzyme Technology
Faculty of Science, Mahidol University
272 Rama VI Road, Ratchathewi, Bangkok, 10400 (Thailand)

[f] Dr. H. J. Wijma, Prof. Dr. M. W. Fraaije
Molecular Enzymology Group
Groningen Biomolecular Sciences and Biotechnology Institute
University of Groningen
Nijenborgh 4, 9747 AG Groningen
(The Netherlands)

[g] Asst. Prof. Dr. N. Lawan
Department of Chemistry, Faculty of Science, Chiang Mai University
239 Huaykaew Road, Suthep, Chiang Mai, 50200 (Thailand)

Supporting information and the ORCID identification numbers for the authors of this article can be found under https://doi.org/10.1002/cbic.201900737.

obtain variants with significantly increased thermostability ($\Delta T_m > 5–10\,^{\circ}C$).[10] The *B* factor iterative test (B-FIT) has been shown to be a promising method for protein engineering. This methodology aims to rigidify the most flexible residues in a protein and has been employed as a semirational strategy to improve the thermostabilities of several enzymes.[11–15] Nevertheless, thousands of clones must be constructed for screening, and many stabilized mutations are missed if the targeted residues with high *B* factors are not located in the most critical regions for stability.[16] Computational design has become feasible as a rational-design method to improve thermostability.[17] This technique provides reasonable predictive accuracy and reduces the need for laborious experimental screening. Several methods aim to optimize native state interactions, variously through improving core packing[18–20] or fragment contacts,[21] or by performing combined structure- and phylogeny-guided energy optimization,[22,23] surface-charge optimization,[24,25] and rigidification.[16,26] Many computational approaches directed towards predicting the stabilizing effects of mutations, such as the FoldX[27] and Rosetta[28] algorithms, have been developed.

The reductase component (C_1) of a two-component (4-hydroxyphenyl)acetate (HPA) 3-hydroxylase (HPAH) from *Acinetobacter baumannii* is an NADH:flavin mononucleotide (FMN) oxidoreductase that catalyzes the reduction of FMN by NADH to generate reduced FMN ($FMNH^-$) for its monooxygenase counterpart (C_2) to hydroxylate the HPA substrate for the synthesis of (3,4-dihydroxyphenyl)acetate (DHPA) in the presence of molecular oxygen (Scheme 1).[29–32] In the case of the two-component flavin-dependent monooxygenases, in general, the reduced flavin generated by a flavin reductase must be transferred to a corresponding monooxygenase to complete the hydroxylation reaction. Therefore, key biological processes such as catabolism, detoxification, biosynthesis, and light emission often involve coupled reductase- and monooxygenase-catalyzed reactions.[32,33,35–40]

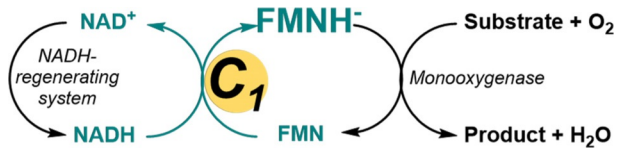

Scheme 1. The C_1-catalyzed reaction that generates $FMNH^-$ for monooxygenase-catalyzed reactions. The NADH-regenerating system might be, for example, glucose/glucose dehydrogenase, glucose 6-phosphate/glucose 6-phosphate dehydrogenase,[41,42] or formate/formate dehydrogenase.[43,44] The monooxygenases might be, for example, C_2 or bacterial luciferase.

C_1 is unique among the flavin reductases in that the HPA substrate can stimulate the rates both of FMN reduction and of $FMNH^-$ release.[30,31,33,34] X-ray structures of FMN-bound C_1 have been solved at 2.2 Å (PDB ID: 5ZYR; Oonanant et al., unpublished results) and 2.9 Å (PDB ID: 5ZC2).[34] The structural analyses indicated that C_1 exists as a homodimer and that each subunit consists of two domains: N- and C-terminal domains (Figure S1). The N-terminal domain (residues 1–169) is a flavin reductase domain that contains tightly bound FMN, whereas the C-terminal domain (residues 190–315) is predicted to be a MarR domain, typically found as a transcription factor. These two domains are linked by a flexible loop (residues 170–189).[33,34] Thanks to its redox reaction generating $FMNH^-$, C_1 has been applied in the enzymatic cascade reactions of the bacterial luciferase (luxAB) from *Vibrio campbellii*[45] and monooxygenase (C_2)[41,42] to produce a bioluminescence signal as a promising eukaryote gene reporter or to synthesize trihydroxyphenolic acids such as 3,4,5-trihydroxycinnamic acid (3,4,5-THCA) and (3,4,5-trihydroxyphenyl)acetic acid (3,4,5-THPA), which are strong antioxidants. However, these reactions were performed only at room temperature, because C_1 is rather unstable at higher temperatures. Therefore, improvement of the thermostability of C_1 is requisite for broad-spectrum uses in the reactions of other two-component flavin-dependent monooxygenases that effect regio- and stereospecific oxygen insertions to produce pharmaceutical ingredients and fine chemicals in industrial applications.[46–49]

In this work we have used in silico approaches—FireProt and FRESCO (framework for rapid enzyme stabilization by computational libraries) programs—to help predict and engineer C_1 variants with greater thermostability. The computational calculations using two protein engineering tools (FoldX and Rosetta), together with energy- and evolution-based calculations, suggested a library of 30 stable C_1 variants. With our screening methods and experimental approaches, only two stable C_1 variants—A166L and A58P—were candidate variants showing improvements in thermostability, with 3–6 °C higher melting temperatures (T_m), and increased catalytic efficiency relative to the WT C_1 enzyme. On heating at 45 °C, both C_1 variants were thermotolerant, with their residual activities retaining about half of their initial values, and still more active than the WT in generating $FMNH^-$ for supply to the reactions catalyzed by luxAB and by C_2. From the lower energy barriers it was inferred that thermostable C_1 variants generate $FMNH^-$ more rapidly than the WT. In addition to thermotolerance, the A166L and A58P variants also exhibited solvent tolerance. The results obtained from molecular dynamics (MD) simulations suggested that mutations of A166 to L and of A58 to P resulted in increased thermostability due to hydrophobic–hydrocarbon interactions between L166 and L168 and between R201 and Q204 and aromatic–hydrocarbon interactions between P58 and F19 and I14. Our results demonstrate that the use of computational calculations helps create stable C_1 variants with improved thermostability and that the rationally designed engineered enzymes also showed increased catalytic efficiency.

Results and Discussion

Use of in silico approaches to predict stable C_1 variants

We used two computational calculation programs—FireProt[23,50] and FRESCO[16,51]—to predict stable C_1 variants. The X-ray structure of the WT C_1 (PDB ID: 5ZYR) was processed with the FireProt program to predict stable variants through a combination of energy- and evolution-based computational approaches.[50] FireProt uses two protein engineering tools, FoldX and Rosetta, to compute the differences in folding free energy

change ($\Delta\Delta G^{fold}$) of the WT ($\Delta G^{fold,WT}$) and variant ($\Delta G^{fold,variant}$) so as to evaluate the folding stability of each variant. $\Delta\Delta G^{fold}$ values of less than -1 kcal mol^{-1} were used to identify the stable variants.[50,52] From the $\Delta\Delta G^{fold}$ values, 15 single-point mutations were predicted as stable candidate variants. Twelve of the stable variants (A18M, N132M, S155P, V167P, A180Y, G186F, V200W, T218W, S219A, Q239M, E248D, and N307Y) were obtained from the energy-based approach, whereas an additional three stable variants (A58P, N106G, and T298S) were obtained from the evolution-based approach (Table S1).

In addition to FireProt, computational prediction by FRESCO, employing energy-based calculation by use of the FoldX and Rosetta tools together with prediction of disulfide bond formation,[16] provided another 15 variants: E10N, E10R, E10Q, A88R, A166D, A166M, A166L, A202W, A221M, A232K, A232Q, A232N, A232H, A243N, and A243G. It should be noted that stable C_1 variants featuring mutations of surface hydrophilic amino acids to hydrophobic side chains should be omitted due to concerns relating to low protein solubility.[51] Altogether, a library of 30 stable mutated C_1 variants was identified.

Thermal screening of the thermostable C_1 variants

Expression constructs harboring each C_1 variant were overexpressed in *Escherichia coli* under optimized conditions as described in the Experimental Section. After cell disruption and debris separation by centrifugation, the crude extracts containing each C_1 variant were heated at 45 °C for 10 min and the clear supernatants were assayed for NADH oxidation activity in the presence of HPA. Reaction progress was monitored for absorbance change at 340 nm. The reaction slope and specific activity for each variant were determined. The specific activities of only ten stable C_1 variants—E10Q, A18M, A58P, N106G, A166L, V200W, A202W, A232K, A232N, and S219A—were higher than or comparable with that of the WT. By this screening method, we were able to narrow down the number of stable C_1 variants showing improved thermostability.

In order to verify the selection of C_1 variants possessing improved thermostability, thermal denaturation of the purified C_1 variants compared to that of the WT was investigated. All ten selected C_1 variants, as well as the WT, were purified to homogeneity by precipitation methods and column chromatography as described in the Experimental Section and the purity of each C_1 variant with the subunit molecular weight (MW) of 35 kDa was assessed by 12% (*w*/*v*) SDS-PAGE (Figure S2). Each of the purified C_1 variants was examined with regard to thermal denaturation by employment of the bound FMN fluorescence-based thermal shift assay by using a real-time polymerase chain reaction (PCR) apparatus with a gradient temperature increase mode.[53,54] The T_m values of C_1 variants and of the WT were determined from the melting curves and are summarized in Table 1. To verify the measured T_m values, two independent batch preparations of each C_1 variant were prepared and multiple T_m measurements were performed. The results in Table 1 indicate that, in relation to that of the WT, only three C_1 variants—A58P, A202W, and A166L—showed significantly higher ΔT_m values (2.6–5.6 °C), thus suggesting that they were highly thermostable, whereas the only slightly increased ΔT_m values (0.3–1.8 °C) of the other variants (E10Q, A232K, A18M, S219A, N106G, and A232N) indicated only moderate thermal stability. On the other hand, the T_m value of the variant V200W was much less than that of the WT, thus indicating significantly lower thermostability. These data demonstrated that prediction of mutation sites with the aid of the computational algorithms of the FireProt and FRESCO programs can provide rationally designed C_1 variants with improved thermostability.

Table 1. Melting temperature (T_m) values of C_1 variants, relative to the WT.

C_1 enzyme	T_m [°C][a]	ΔT_m [°C] [b]	C_1 enzyme	T_m [°C][a]	ΔT_m [°C] [b]
WT	50.7 ± 0.5	0.0	A166L	56.3 ± 1.2	5.6
A202W	55.5 ± 0.8	4.8	A58P	53.3 ± 0.8	2.6
A232N	52.5 ± 0.8	1.8	N106G	52.3 ± 0.8	1.6
S219A	52.0 ± 0.0	1.3	A18M	51.5 ± 0.5	0.8
A232K	51.2 ± 0.4	0.5	E10Q	51.0 ± 0.6	0.3
V200W	47.7 ± 0.5	−3.0			

[a] The S.D. values were calculated from the T_m values obtained from two independent batch preparations and multiple T_m measurements of each C_1 variant. [b] The ΔT_m values were calculated by subtraction of the T_m value of the WT from that of each variant.

Comparison of the NADH oxidation kinetics of selected thermostable C_1 variants relative to the WT

The results in the above section showed that only three candidate C_1 variants—A58P, A202W, and A166L—showed significantly higher thermostability (> 2.0 °C) than the WT. We then investigated the kinetics of NADH oxidation by the bound FMN component in each thermostable C_1 variant at 25 °C in the presence and in the absence of HPA and compared them with those of the WT. The kinetic constants, k_{cat}, K_m, and k_{cat}/K_m, for each thermostable C_1 variant were determined and compared with those of the WT. As shown in Table 2, the k_{cat} values for the reaction catalyzed by the A166L variant in the presence and in the absence of HPA were about 2–3.5 times higher than those of the WT, thus showing that the A166L variant catalyzes the reaction more effectively than the WT. Concurrently, the reaction catalyzed by the A58P variant showed k_{cat} values similar to those of the WT. On comparison of the k_{cat}/K_m values, which represent the catalytic efficiency of NADH

Table 2. Comparison of the catalytic efficiency of thermostable C_1 variants in relation to the WT.

C_1 enzyme	−HPA[a]			+HPA[a]		
	k_{cat} [s^{-1}]	K_m [μM]	k_{cat}/K_m [$\mu M^{-1} s^{-1}$]	k_{cat} [s^{-1}]	K_m [μM]	k_{cat}/K_m [$\mu M^{-1} s^{-1}$]
WT	13.3	9.1 ± 1.6	1.5	164.9	65.4 ± 5.7	2.5
A166L	46.0	32.8 ± 9.9	1.4	345.3	131.8 ± 10.5	2.6
A202W	0.1	10.7 ± 5.5	0.0093	0.4	0.4 ± 0.1	1.0
A58P	17.0	5.8 ± 0.9	2.9	181.0	30.9 ± 5.1	5.8

[a] The reaction assays were performed at 25 °C.

oxidation activity of C_1, the A58P variant showed k_{cat}/K_m values about twice those of the WT in the presence and in the absence of HPA, whereas the A166L variant showed values comparable to those of the WT. The kinetic data suggested that both the A166L and the A58P variants were potentially more suitable candidates than the WT for biocatalysis applications because they can generate the $FMNH^-$ much more rapidly. In contrast to those catalyzed by the A166L and A58P variants, the reactions catalyzed by the A202W variant in the presence and in the absence of HPA showed very low k_{cat} and k_{cat}/K_m values, thus implying that this variant has a much lower turnover and catalytic efficiency for NADH oxidation, and thus shows decelerated generation of the $FMNH^-$.

Thermotolerance of selected thermostable C_1 variants

The work described in the previous sections suggested that only the A58P and the A166L C_1 variants exhibited reasonable improvements in T_m and catalytic efficiency relative to the WT. In order to investigate further whether the two selected thermostable C_1 variants were indeed thermotolerant, time-course heat treatment of the C_1 variants was performed and the residual NADH oxidation activity of each C_1 variant in the presence or in the absence of HPA was measured and compared with that of the WT. Because the T_m values of the WT and of the A58P and A166L enzymes were 50.7, 53.3, and 56.3 °C, respectively (Table 1), an incubation temperature of 45 °C was chosen; at this temperature each of the C_1 variants should still be active for a certain period during incubation. After incubation at 45 °C for various time periods (0–180 min), the data obtained from the reaction in the absence of HPA (Figure 1 A) indicated that only the A58P variant showed a reasonable residual activity, of about 33 % of its initial activity, after incubation for 180 min. Meanwhile, the residual activities both of the A166L variant and of the WT were decreased drastically, retaining only about 7 % of their initial activity after only 5 to 10 min incubation. In contrast with the reaction in the absence of HPA, the residual activities in the presence of HPA for both C_1 variants showed retention of as much as 50 % of their initial activity after 180 min incubation, whereas the WT enzyme retained only about 15 % of its initial activity (Figure 1 B).

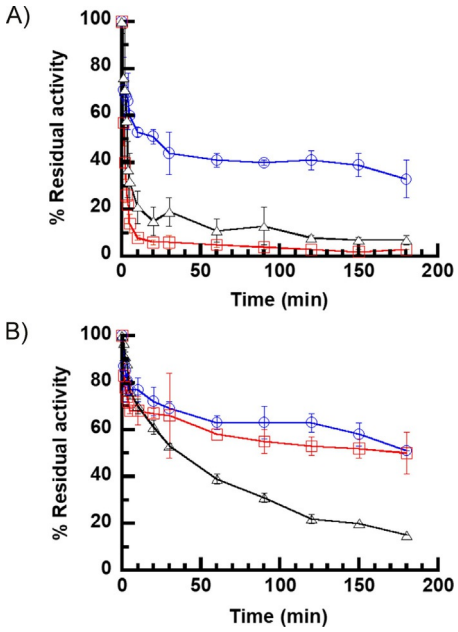

Figure 1. Time-course thermotolerance of C_1 variants, relative to the WT, at 45 °C. The relative residual activity of each C_1 variant (A58P, ○, and A166L, □) was measured and compared to that of the WT (△) in A) the absence, or B) the presence of HPA at 45 °C. Error bars represent S.D.s.

All of these results demonstrated that, in the presence of HPA, both A58P and A166L C_1 variants were thermotolerant and feasible candidates for further uses in biocatalysis applications at high temperature (see later results). Furthermore, the results indicated that the binding of HPA to each C_1 variant can enhance thermotolerance. This could be explained in terms of the influence of a substantial conformational change in the C_1 variant upon HPA binding at the C-terminal domain.[34] Similarly enhanced structural stabilization upon ligand binding has also been observed in the cases of many other enzymes.[55–57] The data obtained also verified that the use of FireProt and FRESCO programs can aid rational design of C_1 variants with improved thermostability.

Generation of the reduced FMN by thermostable C_1 variants has a lower barrier energy than in the case of the WT

On the basis of the steady-state kinetics of NADH oxidation at 25 °C, it had been shown that the overall catalysis by both the A58P and the A166L C_1 variants was faster than that by the WT (Table 2). Hence, we hypothesized that the C_1-bound FMN reduction by NADH could be altered through temperature changes. The transient kinetics of C_1-bound FMN reduction by NADH under anaerobic conditions at various temperatures were studied by stopped-flow spectrophotometry with monitoring at 458 nm. The kinetic traces upon changes in temperature were analyzed for each C_1 enzyme reaction (Figure S3). The results indicated that, at all temperatures employed in all C_1 enzyme reactions, the bound FMN reduction kinetics were biphasic, with both fast and slow flavin reduction. This is similar to the previous report.[31] In this case, only the apparent rate constants of the fast reduction kinetics (k_{red}) were determined, because the amplitude change at 458 nm mainly accounted for about 80 % of overall flavin reduction (Figure S3). The Eyring plots of k_{red} versus different temperatures were analyzed for each C_1 variant (Figure 2). The curve plot showed that the k_{red} values for reduction in the presence of each C_1 variant increased exponentially as the temperature was increased to 50 °C (Figure 2 A).

To obtain the enthalpy of activation ($\Delta H^{\neq}$) of each C_1 reaction, the linear form of the Eyring plot was analyzed (Figure 2 B). The $\Delta H^{\neq}$ values for the A58P and the A166L variants were calculated to be 13.2 and 12.7 kcal mol^{-1}, respectively, and hence 0.5 and 1.0 kcal mol^{-1} lower, respectively, than that of the WT (13.7 kcal mol^{-1}). The data showed that the energy barriers for generation of the reduced flavin in the presence of the thermostable C_1 variants were lower than that of the WT, thus implying that the selected thermostable C_1 variants can

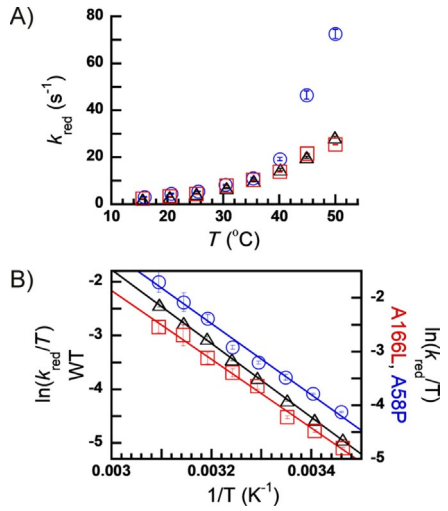

Figure 2. Effects of temperature on generation of the reduced flavin through the action of thermostable C_1 variants relative to the WT. A) Exponential forms of Eyring plots of the apparent rate constants of the fast reduction kinetics (k_{red}) versus various temperatures (15 to 50 °C) for A58P (○) and A166L (□), in comparison with WT (△). B) Linear forms of Eyring plots of k_{red}/T versus $1/T$. The enthalpies of activation ($\Delta H^{\neq}$) of the A58P and A166L variants were calculated to be 13.2 and 12.7 kcal mol^{-1}, respectively, 0.5 and 1.0 kcal mol^{-1} lower, respectively, than that of the WT (13.7 kcal mol^{-1}). Error bars represent S.D.s.

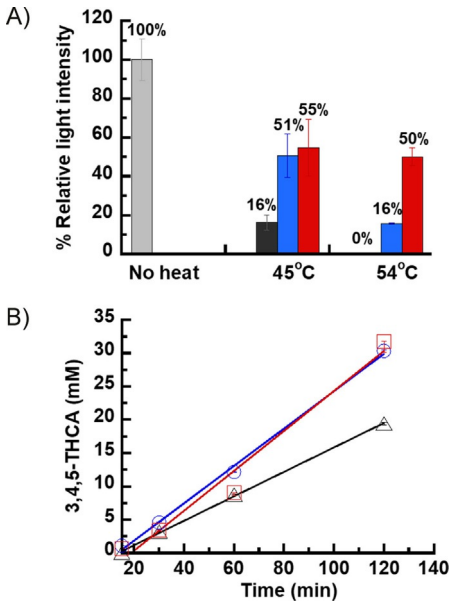

Figure 3. The use of thermostable C_1 variants for A) FMNH$^-$ generation for bioluminescence, and B) production of 3,4,5-THCA. A) The % relative light intensities obtained from luxAB-catalyzed reactions in the presence of C_1 WT (black) and the A58P (blue) and A166L (red) variants heated at 45 or 54 °C compared to that obtained from the reaction in the presence of unheated C_1 WT (gray). B) 3,4,5-THCA produced over time in the multiple turnover reactions catalyzed by the C_2 Y398S mutant in the presence of the C_1 WT (black line with triangles) and the A58P (blue line with circles) and A166L (red line with squares) variants heated at 45 °C to produce FMNH$^-$. Error bars represent S.D.s.

produce the reduced flavin more rapidly, which is suitable for biocatalysis applications (see next results).

Evidence showing that thermostable C_1 variants are effective biocatalysts for supplying the reduced flavin for bioluminescence and for bioactive compound synthesis at high temperatures

Previous studies had demonstrated that the reaction catalyzed by the C_1 WT can supply the reduced flavin for the reactions of flavin-dependent monooxygenases such as the HPAH oxygenase component C_2 for a one-pot synthesis of 3,4,5-THCA[41,42] or of the bacterial luciferase luxAB for generation of bioluminescence.[45,58] Therefore, to investigate whether the two selected thermostable C_1 variants were more effective than the WT in supplying the reduced flavin for the C_2- and luxAB-catalyzed reactions, the C_1 variants and WT enzymes were subjected to preheating at 45 and 54 °C prior to the reaction. It should be noted that only the C_1 enzymes heated to 45 °C were used in the C_2-catalyzed reaction (see details in Experimental Section).

The results shown in Figure 3 A illustrated that the luxAB-catalyzed reaction in the presence of the C_1 variants heated to 45 °C showed a bioluminescence signal about half that of the reaction in the presence of unheated C_1 WT, whereas the bioluminescence signal obtained from the reaction in the presence of the heated C_1 WT showed a signal only about 16% of that performed in the presence of unheated C_1 WT. With the C_1 enzymes heated at 54 °C, the bioluminescence signal obtained from a luxAB-catalyzed reaction in the presence of the heated A166L variant was still half that of the reaction in the presence of unheated C_1 WT, whereas in the reaction in the presence of the heated A58P variant it was reduced to 16%. In contrast, no significant bioluminescence signal was detected in the reaction in the presence of heated C_1 WT. The data indicated that the two thermostable C_1 variants are thermotolerant and can be used as efficient means of FMNH$^-$ generation in luciferase-based eukaryotic gene reporter assays at physiological temperature (37 °C) and even at higher temperatures.[45,58]

For the synthesis of 3,4,5-THCA—a bioactive compound possessing a variety of biological activities including antibacterial,[59] anti-inflammatory,[60–63] and antivenom[64]—with the aid of the C_2-catalyzed reaction, the results in Figure 3 B showed that the rates of 3,4,5-THCA product formation in the reactions involving both heated C_1 variants (0.28 and 0.30 μM min^{-1} for the A58P and the A166L variant, respectively) were each about twice as fast as than that achieved with the heated C_1 WT (0.18 μM min^{-1}). The results showed that the increased rate of 3,4,5-THCA product formation in the C_2-catalyzed reaction in the presence of both C_1 variants was due to their thermotolerant property that promotes their abilities to generate the reduced flavin more rapidly. The data suggested that both thermostable C_1 variants are promising efficient biocatalysts for providing the reduced flavin for the synthesis of other valuable fine chemicals through catalysis by flavin-dependent monooxygenases. Altogether, the results obtained from both the luxAB- and the C_2-catalyzed reactions demonstrate that improvement of thermostability can enhance C_1 enzymes as robust biocatalysts for biotechnology applications.

Thermostable C_1 variants exhibit solvent tolerance

In order to examine whether thermostable C_1 variants show solvent tolerance, the NADH oxidation activities of the solvent-treated thermostable C_1 variants and of the WT were measured and compared. Each C_1 enzyme was immersed in organic solvents—DMSO, MeOH, and EtOH—at different concentrations at 25 °C prior to the NADH oxidation activity assay (see details in Experimental Section). The results, given in Figure 4, show that at 10% (*v*/*v*) of every solvent used for treating all of the C_1 enzymes, the relative NADH oxidation activity of all treated C_1 enzymes was unchanged in relation to that of each untreated C_1. When the solvent concentration was increased to 30% (*v*/*v*), the relative activity of both thermostable C_1 variants treated with DMSO were slightly reduced (5% reduction), whereas the C_1 WT activity was reduced to 83% (Figure 4A). In the case of MeOH-treated C_1 (Figure 4B), only the relative activity of the A166L variant was found to be unchanged, whereas that of the A58P variant was reduced to 70%, and that of the WT was drastically decreased (70% reduction). In the case of EtOH-treated C_1 (Figure 4C), it was found that only about 30% activity of the A166L variant was detected, whereas the activities of the A58P variant and the WT were almost abolished. The results indicated that the A166L variant is tolerant, to some degree, to all solvents used, at concentrations up to 30% (*v*/*v*). The ability of the A166L variant to resist all solvents could be due to the mutation of A166 to L resulting in an alteration of the overall conformation of the C_1 variant, thus preventing solvent accessibility. These data indicated that the A166L C_1 variant might have potential for further development as a robust redox biocatalyst for solvent-dependent synthesis of fine chemicals.

Use of MD simulations to explain the thermostability improvement in C_1 variants

As demonstrated in the preceding sections, our results revealed that A166L and A58P C_1 variants are thermostable and solvent-tolerant enzymes that could effectively generate the reduced flavin for the reactions catalyzed by luxAB and by C_2. To explain why single-point mutations of A166 to L and of A58 to P can improve the thermostability of the C_1 enzyme, we performed MD simulations on the two thermostable C_1 variants for comparison with the WT so as to investigate the plausible roles of these mutated residues that might help stabilize the protein structure and be involved in flavin reactivity. MD was used to investigate the possible interactions engaged in by A166 or A58 and nearby residues that might help stabilize the protein structure under elevated temperatures. Analysis of the C_1 structure (PDB ID: 5ZYR) shows that A166 is near L168, R201, and Q204 (Figure 5 and S4) and that A58 is near I14 and F19 (Figure 6 and S5). Therefore, the distances between the C_α atoms of the residue pairs (A166/L166 and L168, A166/L166 and R201, A166/L166 and Q204, A58/P58 and I14, and A58/P58 and F19) were monitored over MD simulations of 6 ns at 300–500 K.

The results obtained from the MD simulations showed that increasing temperature caused all distances to increase in the case of the WT (Figures 5, 6, S4, and S5). In the cases of the A166L and A58P variants, however, all five distances between C_α of the residue pairs were stable and did not increase with temperature (Figures 5, 6, S4, and S5). This result indicated that these variants were more thermostable than the WT. The thermostability of the A166L variant was improved due to hydrophobic–hydrocarbon interactions between L166 and L168 and between R201 and Q204 (Figures 5 and S4). Mutation of amino acid residues with a shorter aliphatic side chain (Ala) to ones with a longer, bulkier side chain (Leu) on the surface of a chain region is more likely to generate beneficial mutants due to the formation of strong linkages, maximizing contacts with the inner chain, and minimizing entropy effects. The mutation A166L evidently increased hydrophobic interactions at the interface between the subunits, and this stabilized the quaternary structure at higher temperatures without decreasing the specific activity. In the case of the A58P variant, the thermostability improvement was due to aromatic–hydrocarbon interactions between P58 and F19 and I14 (Figures 6 and S5).

Conclusions

This study used in silico approaches to rationally design variants of the reductase component (C_1) of (4-hydroxyphenyl)acetate 3-hydroxylase (HPAH) with improved thermostability. According to the employed experimental approaches, two C_1 variants—A166L and A58P—were found to possess greater thermostability with increased T_m values and greater catalytic efficiency in relation to the WT enzyme. Both thermostable C_1 variants remained active after preheating at 45 °C and were

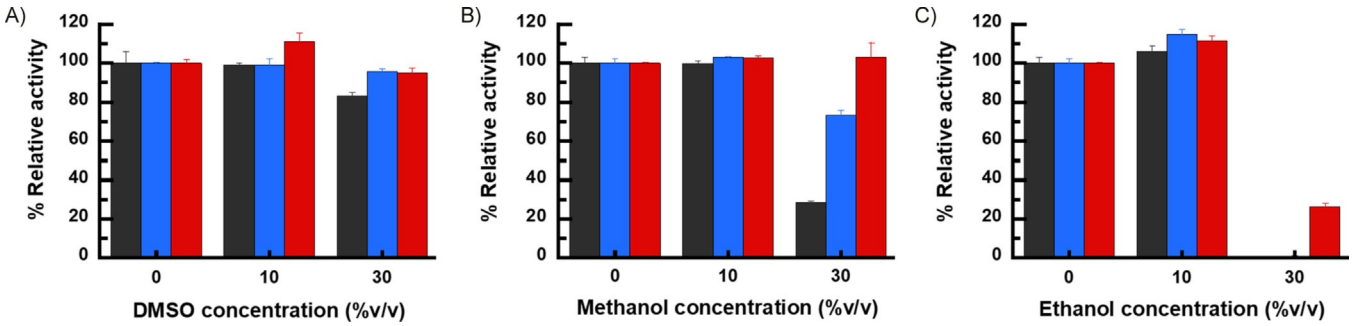

Figure 4. Relative solvent-tolerant NADH oxidation activity of thermostable C_1 variants compared to the WT. Relative activity of C_1 WT (black), A58P (blue), and A166L (red) pretreated with different concentrations (0, 10, and 30%, *v*/*v*) of A) DMSO, B) MeOH, and C) EtOH. Error bars represent S.D.s.

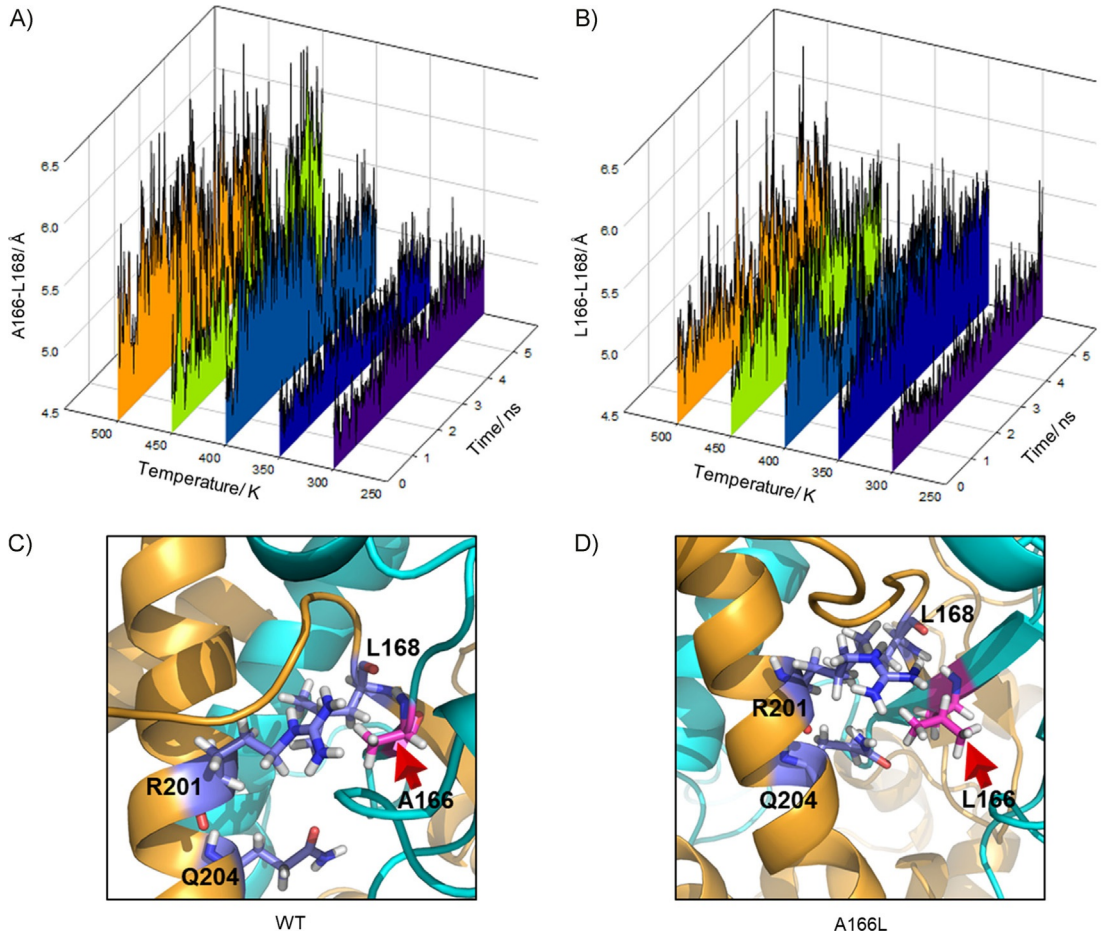

Figure 5. Distances between A166/L166 and L168: A) in the wild type, and B) in the A166L variant over 6 ns MD simulation, at temperatures varying from 300–500 K. Interactions between A166/L166 of C) the wild type, and D) the A166L variant and other residues after 6-ns MD simulations.

able to generate the reduced flavin ($FMNH^-$) for the reactions catalyzed by bacterial luciferase (luxAB) and by monooxygenase C_2. The energy barriers for $FMNH^-$ generation in the cases of both thermostable C_1 variants were lower than those in that of the WT enzyme, thus implying that both variants could produce $FMNH^-$ more rapidly than the WT. In addition to thermostabilty, both C_1 variants also exhibited solvent tolerance. This was especially evident with the A166L variant, which remained active after pretreatment with 30% (*v*/*v*) DMSO, methanol, and ethanol. MD simulations at a high temperature indicated that the single-point mutations of A166 to L and of A58 to P could maintain the distances around those residues through hydrophobic– and aromatic–hydrocarbon interactions, respectively, resulting in thermostability improvements in both C_1 variants.

Experimental Section

Chemicals: All chemicals and reagents used were of analytical grade and commercially available. PCR primers were synthesized by HAP Oligo Synthesis (Bio Basic, Inc., USA). Concentrations of the following compounds were calculated on the basis of known extinction coefficients at pH 7.0: NADH has $\varepsilon_{340} = 6.22\ mM^{-1}\ cm^{-1}$, HPA has $\varepsilon_{277} = 1.55\ mM^{-1}\ cm^{-1}$, FMN has $\varepsilon_{446} = 12.2\ mM^{-1}\ cm^{-1}$, C_1 has $\varepsilon_{458} = 12.8\ mM^{-1}\ cm^{-1}$, and C_2 has $\varepsilon_{280} = 56.7\ mM^{-1}\ cm^{-1}$.[30–33] *p*-Coumaric acid (CMA) has $\varepsilon_{285} = 16.92\ mM^{-1}\ cm^{-1}$, caffeic acid (CFA) has $\varepsilon_{312} = 9.42\ mM^{-1}\ cm^{-1}$, and 3,4,5-THCA has $\varepsilon_{300} = 12.7\ mM^{-1}\ cm^{-1}$.[42]

In silico methods for design of C_1 variants: The thermostable C_1 variants were predicted by using two computational programs: FireProt[23,50] and FRESCO.[16,51] The dimeric structure of C_1 WT (PDB ID: 5ZYR) was processed with the aid of the FireProt program, which uses FoldX and Rosetta tools for calculation of the $\Delta\Delta G^{fold}$ values that indicate folding stability. Only the C_1 variants with $\Delta\Delta G^{fold}$ values lower than $-1\ kcal\,mol^{-1}$ were selected for further studies and analyses. The prediction with the aid of the FRESCO program was performed along with energy-based calculation by using the FoldX and Rosetta tools and prediction of disulfide bond formation.[16]

Site-directed mutagenesis: The pET11a-C_1 plasmid was used as a template for site-directed mutagenesis to generate all C_1 variants. The PCR protocol was described in previous reports,[30,33] and the forward and reverse primers used for PCR reactions are shown in Table S2. The PCR reaction mixture contained 1× Pfu buffer with $MgSO_4$ (20 mM), each dNTP (0.4 mM), forward and reverse primers (0.4 mM), Pfu DNA polymerase (2.5 U), and template (1 μg). The PCR conditions were as follows: preheating of the reaction mixture to 95 °C for 5 min, followed by 30 cycles of denaturation at 95 °C for 30 s, annealing at 45–65 °C for 30 s, and elongation at 72 °C for 14 min. A final extension was carried out at 72 °C for 10 min. The amplified products were analyzed on agarose gels (1%), and the

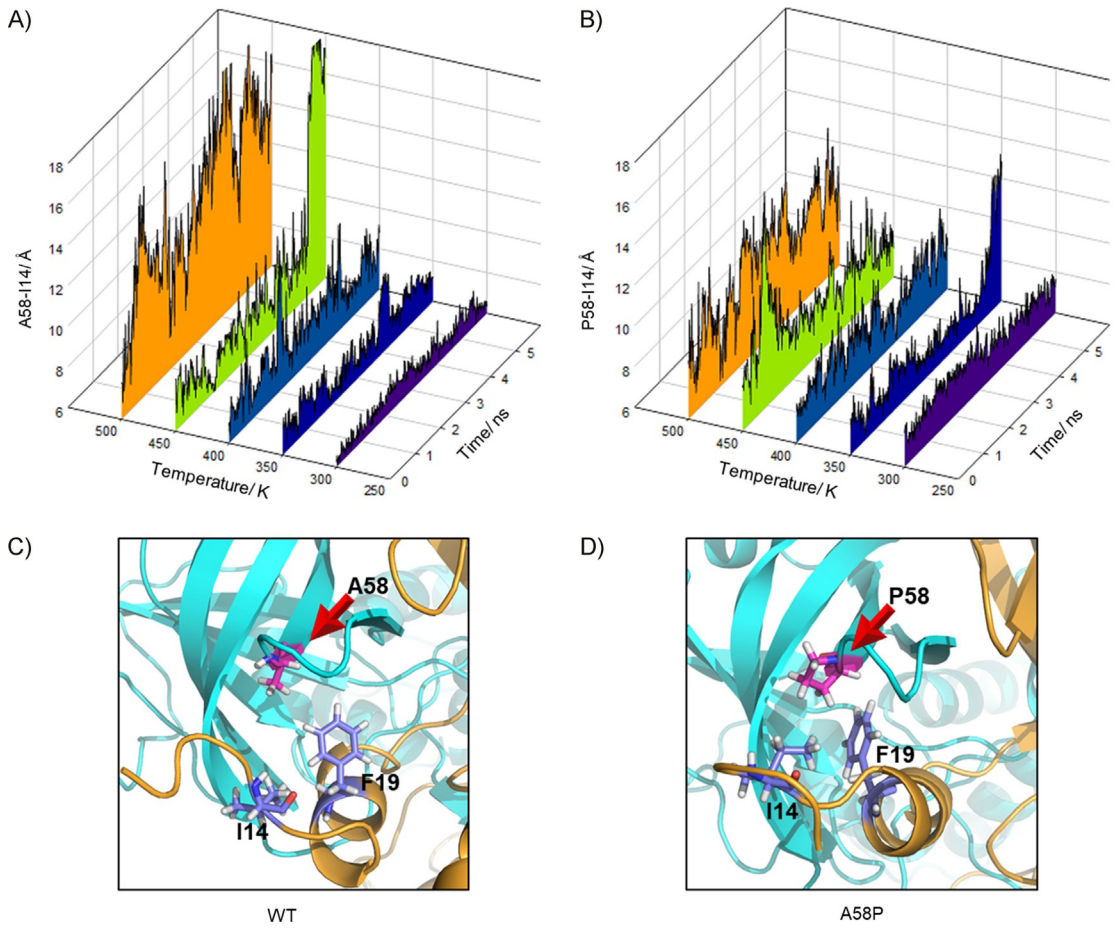

Figure 6. Distances between A58/P58 and I14: A) in the wild type, and B) in the A58P variant over 6 ns MD simulation, at temperatures varying from 300–500 K. The interactions between A58/P58 of C) the wild type, and D) the A58P variant and other residues after 6-ns MD simulations.

expected product size was approximate 6.6 kbp. The template was digested with DpnI (20 U) for 1 h at 37 °C (New England Biolabs). Plasmids encoding for the C_1 variants were propagated in *E. coli* XL1-Blue and purified according to the FavorPrep Plasmid DNA extraction Mini Kit protocols (Favorgen Biotech Corporation, Ping-Tung, Taiwan). All plasmids were analyzed for their sequences at 1st BASE DNA Sequencing Services (Malaysia).

Protein expression and purification: The protocol for C_1 enzyme expression in *E. coli* BL21(DE3) was established and described in previous reports.[30,33] Protein purification was carried out according to the previous protocol[29,30,33] with slight modifications. In brief, the crude extract of each C_1 enzyme was purified to homogeneity by precipitation methods by using polyethylenimine (1%, *w/v*) to remove nucleic acid contents and ammonium sulfate (20–40%, *w/v*) to fractionate C_1 enzyme, as well as anion-exchange chromatography with a DEAE-Sepharose column at pH 7.0. The purified C_1 enzyme was kept in MOPS buffer (pH 7.0, 100 mM) and stored at −80 °C until use. The purity of each C_1 enzyme was estimated by SDS-PAGE analysis (12%, *w/v*) and the amount of protein was quantitated by use of the Bradford assay. The stock C_1 enzyme concentration was determined by using the molar absorption coefficient of bound FMN at 458 nm ($\varepsilon_{458} = 12.8\ mM^{-1}\ cm^{-1}$).

Measurement and kinetics of NADH oxidase activity: NADH oxidase activity of the C_1 enzyme was measured by monitoring the absorbance decrease at 340 nm with a Cary 100 UV/Vis spectrophotometer (Agilent, USA). A typical assay reaction contained C_1 (4–16 nM), FMN (15 μM), and NADH (200 μM) in sodium phosphate buffer (pH 7.0, 50 mM) at 25 °C. Because C_1 activity can be stimulated by HPA,[29–31,33] the assay reactions were carried out in the presence of HPA for comparison with those performed in the absence of HPA. Basal NADH oxidase activity was measured before the start of the reaction by addition of HPA (200 μM). Therefore, the specific NADH oxidation in the presence of C_1 was calculated by subtracting the basal NADH oxidase activity from the total NADH oxidation. One unit of C_1 activity is defined as the amount of enzyme required to oxidize 1 μmol of NADH per min under the assay conditions. For NADH oxidase kinetics, various concentrations of NADH (1–400 μM) were added to the triplicate assay reaction mixtures. The initial rates (v) of the reactions were calculated and plotted versus NADH concentrations. The curve plots were fitted by the Michaelis–Menten equation [Eq. (1)], in which v_{max} is the maximum rate, K_m is the Michaelis constant for substrate S, and S is the [NADH], by using the Levenberg–Marquardt algorithm in KaleidaGraph version 4.0 software (Synergy Software) to determine the kinetic parameters.

$$v = \frac{v_{max} S}{K_m + S} \quad (1)$$

Screening for thermostable C_1 variants: A clear solution of a crude extract of a C_1 variant or WT was incubated in a water bath heated at 45 °C for 10 min. After incubation, the pellet was separated by centrifugation. The protein content of the clear supernatant

was determined by Bradford assay and the NADH oxidation activity was measured by spectrophotometry as described above. The specific activity of each C_1 variant was compared with that of the WT enzyme. The C_1 variants that had greater specific activity than the WT were selected for further characterization.

Thermostability assay: Time-dependent thermal inactivation assays of C_1 enzymes were examined for evaluation of the enzyme thermotolerance. Each C_1 variant was incubated in a water bath heated at 45 °C for various incubation times (0–180 min). At each timepoint, an aliquot of C_1 solution was taken and then added into the assay reaction to measure NADH oxidation activity in the absence and in the presence of HPA as described earlier. The residual activity of C_1 at each timepoint was calculated and compared.

Thermal denaturation: A melting curve analysis of each C_1 variant was conducted to determine the thermal unfolding temperature (T_m),[65] by monitoring of the increase in the intrinsic fluorescence of bound FMN upon thermal protein denaturation.[54] A C_1 sample (5 μM) was mixed with sodium phosphate buffer (pH 7.0, 50 mM) in a total volume of 20 μL in a PCR tube. The intrinsic fluorescence signal was monitored while the temperature was increased from 25 to 90 °C at a constant increment of 1 °C min^{-1} in an CFX96 real-time PCR instrument (BIO-RAD, United Kingdom). The protein melting curve plot of intrinsic fluorescence signal versus temperature was analyzed and used for determining the T_m value, the temperature at which half of the total protein is in the unfolded state.[66] Alternatively, the melting curve plot can be transformed to the first derivative plot of $-dF/dT$ versus temperature [°C], in which the T_m values correspond to peaks.[67]

Effect of temperature on transient kinetics of thermostable C_1-bound FMN reduction by NADH: Rate constants of flavin reduction at various temperatures were measured according to the procedure described previously.[68–71] In brief, the measurements were performed with a TgK Scientific Model SF-61DX stopped-flow spectrophotometer in single-mixing mode. The stopped-flow apparatus was made anaerobic by flushing the flow system with an oxygen scrubbing solution containing glucose (20 mM) and glucose oxidase (10 units). The oxygen scrubbing solution was allowed to stand in the flow system overnight and the system was thoroughly rinsed with the anaerobic buffer before experiments.

A solution (25 μM) of C_1 WT or variant was mixed with NADH (100 μM, concentrations after mixing) at various temperatures (15, 20, 25, 30, 35, 40, 45, and 50 °C) in a stopped-flow apparatus. The absorbance changes at 458 nm were monitored. The apparent rate constant of flavin reduction (k_{red}) was calculated from the kinetic traces by use of exponential fits and the software packages of Kinetic Studio (TgK Scientific, Bradford-on-Avon, UK) or Program A (developed by R. Chang, C.-J. Chiu, J. Dinverno, and D. P. Ballou, at the University of Michigan, Ann Arbor, MI). The exponential curve of k_{red} versus temperatures was plotted and analyzed by use of the Eyring equation [Eq. (2)], in which k_B is the Boltzmann constant (1.381×10^{-23} J K^{-1}), h is Planck's constant (6.626×10^{-34} J s), T is the absolute temperature, R is the gas constant (1.987 cal mol^{-1} K^{-1}), $\Delta H^{\neq}$ is the enthalpy of activation, and $\Delta S^{\neq}$ is the entropy of activation.[72] The linear form of the Eyring plot of $\ln(k_{red}/T)$ versus $1/T$ was analyzed by using Equation 3 to determine the enthalpy of activation ($\Delta H^{\neq}$) from the slope of the plot.

$$k = \left(\frac{k_B T}{h}\right) \times e^{\left(\frac{-\Delta H^{\neq}}{RT}\right)} \times e^{\left(\frac{-\Delta S^{\neq}}{R}\right)} \quad (2)$$

$$\ln\frac{k}{T} = -\frac{-\Delta H^{\neq}}{R}\frac{1}{T} + \ln\frac{k_B}{h} + \frac{-\Delta S^{\neq}}{R} \quad (3)$$

Measurement of in vitro bioluminescence by using thermostable C_1 variants as electron donors for bacterial luciferase activity: A bacterial luciferase (luxAB) assay solution (100 μL) consisting of FMN (10 μM), HPA (200 μM), NADH (200 μM), and decanal (20 μM) in sodium phosphate buffer (pH 7.0, 50 mM) was freshly prepared on ice and protected from light.[45] After all reagents had been prepared, the luciferase assay solution was injected into a mixture solution (10 μL) of luxAB (75 fM, 5 μL) and C_1 (50 mU, 5 μL) by using an AB-2270 luminometer (ATTO, Tokyo, Japan). The light signal was integrated over 60 s and recorded at room temperature (25 °C). It should be noted that C_1 variants and WT were preheated at 45 °C for 6 h or at 54 °C for 10 min prior to assay of the luxAB activity. The bioluminescence signal obtained from the luxAB-catalyzed reaction in the presence of the preheated C_1 variants was then compared with that obtained from the reaction in the presence of preheated or unheated WT.

Production of 3,4,5-THCA by using thermostable C_1 variants for generation of the reduced flavin: Previous reports showed that the reaction catalyzed by C_1 WT serves as a source of reduced flavin for the C_2-catalyzed bioconversion of *p*-coumaric acid (CMA) to produce 3,4,5-THCA.[41,42] Therefore, in this experiment, we investigated whether the selected thermostable C_1 variants would exhibit greater efficiency than the WT in producing the reduced flavin for the C_2-catalyzed reaction. The enzymatic cascade bioconversion was carried out similarly to the previous protocols,[41,42] except that the NADH-regenerating system used in this experiment was that based on *Pseudomonas* sp. 101 formate dehydrogenase (*Ps*FDH).[43,44] This is because *Ps*FDH has a rather high T_m value [(66.7 ± 0.5) °C, data not shown]. It should be noted that C_1 variants and WT were preheated at 45 °C for 3 h prior to the bioconversion reaction.

The reaction (10 mL) was carried out in sodium phosphate buffer (pH 7.0, 100 mM) containing sodium formate (20 mM), preheated C_1 (0.1 μM), NAD^+ (400 μM), C_2 Y398S variant (5 μM), FMN (1 μM), CMA (50 μM), and ascorbic acid (1 mM), plus superoxide dismutase (SOD, 50 unit mL^{-1}). The reaction was initiated by addition of *Ps*FDH (1 μM) and performed at 25 °C. During the reaction progress, aliquots (100 μL) were taken at various times (0–2 h) and quenched by addition of an equivalent volume of HCl (0.2 M). The quenched solution was filtered with a Microcon ultrafiltration unit (10 kDa cut-off, Millipore) to obtain the filtrate fraction containing 3,4,5-THCA, which was analyzed by HPLC (Agilent Technologies 1100 or 1260 Infinity series) equipped with a UV/visible diode-array detector (DAD) and quadrupole mass spectrometric detector (MSD). Liquid chromatographic (LC) separation was achieved with a Nova-Pak C_{18} column (Waters Corporation, USA, 150 mm × 3.9 mm i.d., 4 μm). Total run time for LC separation was 30 min with a flow rate of 0.5 mL min^{-1}. Solvents used for separation were formic acid (0.1%, *v*/*v*) in water (eluent A) and formic acid (0.1%, *v*/*v*) in methanol (eluent B). The separation protocol was as follows: a linear gradient increasing from 0–25% eluent B (t = 0–2 min), maintenance at 25% eluent B (t = 2–10 min), a linear gradient increasing from 25–50% eluent B (t = 10–13 min), maintenance at 50% eluent B (t = 13–18 min), a linear gradient decreasing from 50–0% eluent B (t = 18–20 min). After each separation, the column was equilibrated further for 10 min. A volume of 20 μL was injected for all standard reagents and samples. The chromatographic peak with the retention time at 4.6 min for 3,4,5-THCA product were detected at 300 nm by the DAD and the corresponding 195 *m*/*z* was detected with the MSD. A standard curve of various known concentrations of 3,4,5-THCA versus the corresponding peak areas was used to quantitate concentration of the 3,4,5-THCA product formed at

each timepoint. The rate of 3,4,5-THCA product formation in the reaction involving a preheated C_1 variants was determined and compared with that in the reaction involving preheated WT.

Effects of organic solvents on NADH oxidase activity of thermostable C_1 variants: The thermostable C_1 variants and the WT were pretreated with different concentrations (0, 10, 30%, *v/v*) of different types of organic solvents including DMSO, ethanol, and methanol at 25 °C for 3 h. After incubation, the precipitated protein was separated by centrifugation and the clear solution of C_1 was used for the assay as described earlier. The NADH oxidase activities of the thermostable C_1 variants treated with each solvent were compared with those of the WT under the same conditions.

MD simulations: The C_1 enzyme structure (PDB ID: 5ZYR) was obtained from the Protein Data Bank (PDB). Hydrogen atoms of amino acid residues were added by considering results from the propka (http://propka.org).[73] The atom types in the topology files were assigned with the aid of the CHARMM27 parameter set.[74] The structure of the C_1 enzyme was solvated in a cubic box of TIP3P water extending at least 15 Å in each direction from the solute. The dimensions of the solvated system are 98×89×99 Å. MD simulations were carried out by using the NAMD program[75] with simulation protocols adapted from our previous work[52] and NAMD tutorials.[76,77] The simulations were started by minimizing hydrogen atom positions for 3000 steps followed by water minimization for 6000 steps. The system water was heated to 300 K for 5 ps and was then equilibrated for 15 ps. The whole system was minimized for 10000 steps and heated to 300 K for 20 ps. After that, the whole system was equilibrated for 180 ps followed by production stage for 6 ns. Molecular modeling of the WT and of the A58P and A166L variants was investigated. To investigate temperature effect on the enzyme stability, MD simulations were carried out at 300–500 K. Some separations of important residues, as represented by the distances between C_α atoms of the residue pairs A58 and I14, A58 and F19, A166 and R201, and A166 and Q204 were monitored during 6 ns MD simulations.

Acknowledgements

This work was supported by The Thailand Research Fund [grants no. MRG6080234 (to T.W.), MRG5980001 (to S.M.), and RTA5980001 (to P.C.)]. We also thank the Vidyasirimedhi Institute of Science and Technology (VISTEC) for funding support for V.P., P.A., J.P., P.C., and T.W. and Chiang Mai University for N.L.

Conflict of Interest

The authors declare no conflict of interest.

Keywords: biocatalysis · computational chemistry · flavoproteins · reductases · thermostable enzymes

[1] U. T. Bornscheuer, G. W. Huisman, R. J. Kazlauskas, S. Lutz, J. C. Moore, K. Robins, *Nature* **2012**, *485*, 185 – 194.
[2] C. M. Clouthier, J. N. Pelletier, *Chem. Soc. Rev.* **2012**, *41*, 1585 – 1605.
[3] J. D. Bloom, S. T. Labthavikul, C. R. Otey, F. H. Arnold, *Proc. Natl. Acad. Sci. USA* **2006**, *103*, 5869 – 5874.
[4] J. M. Guisan in *Methods in Molecular Biology, Vol. 1051: Immobilization of Enzymes and Cells*, 3rd ed., Humana, Totowa, **2013**, pp. 1 – 13.
[5] R. A. Sheldon, S. van Pelt, *Chem. Soc. Rev.* **2013**, *42*, 6223 – 6235.
[6] V. Stepankova, S. Bidmanova, T. Koudelakova, Z. Prokop, R. Chaloupkova, J. Damborsky, *ACS Catal.* **2013**, *3*, 2823 – 2836.
[7] A. S. Bommarius, M. F. Paye, *Chem. Soc. Rev.* **2013**, *42*, 6534 – 6565.
[8] M. Lehmann, M. Wyss, *Curr. Opin. Biotechnol.* **2001**, *12*, 371 – 375.
[9] K. Steiner, H. Schwab, *Comput. Struct. Biotechnol. J.* **2012**, *2*, e201209010.
[10] C. A. Tracewell, F. H. Arnold, *Curr. Opin. Chem. Biol.* **2009**, *13*, 3 – 9.
[11] M. T. Reetz, J. D. Carballeira, A. Vogel, *Angew. Chem. Int. Ed.* **2006**, *45*, 7745 – 7751; *Angew. Chem.* **2006**, *118*, 7909 – 7915.
[12] S. Wen, T. Tan, H. Zhao, *J. Biotechnol.* **2013**, *164*, 248 – 253.
[13] Y. Xie, J. An, G. Yang, G. Wu, Y. Zhang, L. Cui, Y. Feng, *J. Biol. Chem.* **2014**, *289*, 7994 – 8006.
[14] J. H. Zhang, Y. Lin, Y. F. Sun, Y. R. Ye, S. P. Zheng, S. Y. Han, *Enzyme Microb. Technol.* **2012**, *50*, 325 – 330.
[15] X. F. Zhang, G. Y. Yang, Y. Zhang, Y. Xie, S. G. Withers, Y. Feng, *Sci. Rep.* **2016**, *6*, 33797 – 33808.
[16] H. J. Wijma, R. J. Floor, P. A. Jekel, D. Baker, S. J. Marrink, D. B. Janssen, *Protein Eng. Des. Sel.* **2014**, *27*, 49 – 58.
[17] J. Damborsky, J. Brezovsky, *Curr. Opin. Chem. Biol.* **2014**, *19*, 8 – 16.
[18] S. M. Malakauskas, S. L. Mayo, *Nat. Struct. Biol.* **1998**, *5*, 470 – 475.
[19] A. Korkegian, M. E. Black, D. Baker, B. L. Stoddard, *Science* **2005**, *308*, 857 – 860.
[20] B. Borgo, J. J. Havranek, *Proc. Natl. Acad. Sci. USA* **2012**, *109*, 1494 – 1499.
[21] Y. Li, D. A. Drummond, A. M. Sawayama, C. D. Snow, J. D. Bloom, F. H. Arnold, *Nat. Biotechnol.* **2007**, *25*, 1051 – 1056.
[22] A. Goldenzweig, M. Goldsmith, S. E. Hill, O. Gertman, P. Laurino, Y. Ashani, O. Dym, T. Unger, S. Albeck, J. Prilusky, R. L. Lieberman, A. Aharoni, I. Silman, J. L. Sussman, D. S. Tawfik, S. J. Fleishman, *Mol. Cell* **2016**, *63*, 337 – 346.
[23] D. Bednar, K. Beerens, E. Sebestova, J. Bendl, S. Khare, R. Chaloupkova, Z. Prokop, J. Brezovsky, D. Baker, J. Damborsky, *PLoS Comput. Biol.* **2015**, *11*, e1004556 – e1004575.
[24] A. V. Gribenko, M. M. Patel, J. Liu, S. A. McCallum, C. Wang, G. I. Makhatadze, *Proc. Natl. Acad. Sci. USA* **2009**, *106*, 2601 – 2606.
[25] A. Bjork, B. Dalhus, D. Mantzilas, R. Sirevåg, V. G. Eijsink, *J. Mol. Biol.* **2004**, *341*, 1215 – 1226.
[26] B. Van den Burg, G. Vriend, O. R. Veltman, G. Venema, V. G. Eijsink, *Proc. Natl. Acad. Sci. USA* **1998**, *95*, 2056 – 2060.
[27] R. Guerois, J. E. Nielsen, L. Serrano, *J. Mol. Biol.* **2002**, *320*, 369 – 387.
[28] E. H. Kellogg, A. Leaver-Fay, D. Baker, *Proteins* **2011**, *79*, 830 – 838.
[29] P. Chaiyen, C. Suadee, P. Wilairat, *Eur. J. Biochem.* **2001**, *268*, 5550 – 5561.
[30] K. Thotsaporn, J. Sucharitakul, J. Wongratana, C. Suadee, P. Chaiyen, *Biochim. Biophys. Acta* **2004**, *1680*, 60 – 66.
[31] J. Sucharitakul, P. Chaiyen, B. Entsch, D. P. Ballou, *Biochemistry* **2005**, *44*, 10434 – 10442.
[32] J. Sucharitakul, T. Phongsak, B. Entsch, J. Svasti, P. Chaiyen, D. P. Ballou, *Biochemistry* **2007**, *46*, 8611 – 8623.
[33] T. Phongsak, J. Sucharitakul, K. Thotsaporn, W. Oonanant, J. Yuvaniyama, J. Svasti, D. P. Ballou, P. Chaiyen, *J. Biol. Chem.* **2012**, *287*, 26213 – 26222.
[34] A. Yuenyao, N. Petchyam, N. Kamonsutthipaijit, P. Chaiyen, D. Pakotiprapha, *Arch. Biochem. Biophys.* **2018**, *653*, 24 – 38.
[35] J. Sucharitakul, R. Tinikul, P. Chaiyen, *Arch. Biochem. Biophys.* **2014**, *555*, 33 – 46.
[36] P. Pimviriyakul, P. Chaiyen, *J. Biol. Chem.* **2018**, *293*, 18525 – 18539.
[37] R. Tinikul, W. Pitsawong, J. Scharitakul, S. Nijvipakul, D. P. Ballou, P. Chaiyen, *Biochemistry* **2013**, *52*, 6834 – 6843.
[38] P. Chenprakhon, T. Wongnate, P. Chaiyen, *Protein Sci.* **2019**, *28*, 8 – 29.
[39] U. Kirchner, A. H. Westphal, R. Müller, W. J. van Berkel, *J. Biol. Chem.* **2003**, *278*, 47545 – 47553.
[40] T. Heine, W. J. H van Berkel, G. Gassner, K. H. van Pée, D. Tischler, *Biology (Basel)* **2018**, *7*, 42 – 76.
[41] T. Dhammaraj, A. Phintha, C. Pinthong, D. Medhanavyn, R. Tinikul, P. Chenprakhon, J. Sucharitakul, N. Vardhanabhuti, C. Jiarpinitnun, P. Chaiyen, *ACS Catal.* **2015**, *5*, 4492 – 4502.
[42] C. Pinthong, P. Phoopraintra, R. Chantiwas, T. Pongtharangkul, P. Chenprakhon, P. Chaiyen, *Process Biochem.* **2017**, *63*, 122 – 129.
[43] A. S. Bommarius, M. Schwarm, K. Stingl, M. Kottenhahn, K. Huthmacher, K. Drauz, *Tetrahedron: Asymmetry* **1995**, *6*, 2851 – 2888.

[44] V. I. Tishkov, A. G. Galkin, G. N. Marchenko, O. A. Egorova, D. V. Sheluho, L. B. Kulakova, L. A. Dementieva, A. M. Egorov, *Biochem. Biophys. Res. Commun.* **1993**, *192*, 976 – 981.
[45] R. Tinikul, K. Thotsaporn, V. Taveekarn, S. Jitrapakdee, P. Chaiyen, *J. Biotechnol.* **2012**, *162*, 346 – 353.
[46] H. Leisch, K. Morley, P. C. Lau, *Chem. Rev.* **2011**, *111*, 4165 – 4222.
[47] S. Schmidt, C. Scherkus, J. Muschiol, U. Menyes, T. Winkler, W. Hummel, H. Groger, A. Liese, H. G. Herz, U. T. Bornscheuer, *Angew. Chem. Int. Ed.* **2015**, *54*, 2784 – 2787; *Angew. Chem.* **2015**, *127*, 2825 – 2828.
[48] Y. Zhu, Q. Zhang, S. Li, Q. Lin, P. Fu, G. Zhang, H. Zhang, R. Shi, W. Zhu, C. Zhang, *J. Am. Chem. Soc.* **2013**, *135*, 18750 – 18753.
[49] F. Hollmann, K. Hofstetter, T. Habicher, B. Hauer, A. Schmid, *J. Am. Chem. Soc.* **2005**, *127*, 6540 – 6541.
[50] M. Musil, J. Stourac, J. Bendl, J. Brezovsky, Z. Prokop, J. Zendulka, T. Martinek, D. Bednar, J. Damborsky, *Nucleic Acids Res.* **2017**, *45*, W393 – W399.
[51] H. J. Wijma, M. J. L. J. Fürst, D. B. Janssen, *Methods Mol. Biol.* **2018**, *1685*, 69 – 85.
[52] P. Pongpamorn, P. Watthaisong, P. Pimviriyakul, A. Jaruwat, N. Lawan, P. Chitnumsub, P. Chaiyen, *ChemBioChem* **2019**, *20*, 3020.
[53] U. B. Ericsson, B. M. Hallberg, G. T. Detitta, N. Dekker, P. Nordlund, *Anal. Biochem.* **2006**, *357*, 289 – 298.
[54] F. Forneris, R. Orru, D. Bonivento, L. R. Chiarelli, A. Mattevi, *FEBS. J.* **2009**, *276*, 2833 – 2840.
[55] M. S. Celej, G. G. Montich, G. D. Fidelio, *Protein Sci.* **2003**, *12*, 1496 – 1506.
[56] S. Vega, O. Abian, A. Velazquez-Campoy, *Biochim. Biophys. Acta* **2016**, *1860*, 868 – 878.
[57] K. Teilum, J. G. Olsen, B. B. Kragelund, *Cell Mol. Life Sci.* **2009**, *66*, 2231 – 2247.
[58] R. Tinikul, P. Chaiyen, *Adv. Biochem. Eng./Biotechnol.* **2016**, *154*, 47 – 74.
[59] V. Srivastava, M. P. Darokar, A. Fatima, J. K. Kumar, C. Chowdhury, H. O. Saxena, G. R. Dwivedi, K. Shrivastava, V. Gupta, S. K. Chattopadhyay, S. Luqman, M. M. Gupta, A. S. Negi, S. P. Khanuja, *Bioorg. Med. Chem.* **2007**, *15*, 518 – 525.
[60] J. W. Lee, C. J. Bae, Y. J. Choi, S. I. Kim, N. H. Kim, H. J. Lee, S. S. Kim, Y. S. Kwon, W. Chun, *Korean J. Physiol. Pharmacol.* **2012**, *16*, 107 – 112.
[61] J. W. Lee, Y. J. Choi, J. H. Park, J. Y. Sim, Y. S. Kwon, H. J. Lee, S. S. Kim, W. Chun, *Biomol. Ther.* **2013**, *21*, 60 – 65.
[62] J. W. Lee, C. J. Bae, Y. J. Choi, S. I. Kim, Y. S. Kwon, H. J. Lee, S. S. Kim, W. Chun, *Mol. Cell. Biochem.* **2014**, *390*, 143 – 153.
[63] R. Nagasaka, C. Chotimarkorn, I. M. Shafiqul, M. Hori, H. Ozaki, H. Ushio, *Biochem. Biophys. Res. Commun.* **2007**, *358*, 615 – 619.
[64] H. T. Aung, T. Furukawa, T. Nikai, M. Niwa, Y. Takaya, *Bioorg. Med. Chem.* **2011**, *19*, 2392 – 2396.
[65] K. Miyazaki, M. Takenouchi, H. Kondo, N. Noro, M. Suzuki, S. Tsuda, *J. Biol. Chem.* **2006**, *281*, 10236 – 10242.
[66] A. Fersht, *Structure and Mechanism in Protein Science: A Guide to Enzyme Catalysis and Protein Folding*, 2nd ed., Freeman, New York, **1999**.
[67] K. Huynh, C. L. Partch, *Curr. Protoc. Protein Sci.* **2015**, *79*, 28.9.1 – 28.9.14.
[68] T. Wongnate, P. Surawatanawong, S. Visitsatthawong, J. Sucharitakul, N. S. Scrutton, P. Chaiyen, *J. Am. Chem. Soc.* **2014**, *136*, 241 – 253.
[69] S. Visitsatthawong, P. Chenprakhon, P. Chaiyen, P. Surawatanawong, *J. Am. Chem. Soc.* **2015**, *137*, 9363 – 9374.
[70] T. Wongnate, D. Sliwa, B. Ginovska, D. Smith, M. W. Wolf, N. Lehnert, S. Raugei, S. W. Ragsdale, *Science* **2016**, *352*, 953 – 958.
[71] T. Wongnate, P. Surawatanawong, L. Chuaboon, N. Lawan, P. Chaiyen, *Chem. Eur. J.* **2019**, *25*, 4460 – 4471.
[72] H. Eyring, *J. Chem. Phys.* **1935**, *3*, 107 – 115.
[73] T. J. Dolinsky, J. E. Nielsen, J. A. McCammon, N. A. Baker, *Nucleic Acids Res.* **2004**, *32*, W665-W667.
[74] A. D. MacKerell, D. Bashford, M. Bellott, R. L. Dunbrack, J. D. Evanseck, M. J. Field, S. Fischer, J. Gao, H. Guo, S. Ha, D. Joseph-McCarthy, L. Kuchnir, K. Kuczera, F. T. K. Lau, C. Mattos, S. Michnick, T. Ngo, D. T. Nguyen, B. Prodhom, W. E. Reiher, B. Roux, M. Schlenkrich, J. C. Smith, R. Stote, J. Straub, M. Watanabe, J. Wirkiewicz-Kuczera, D. Yin, M. Karplus, *J. Phys. Chem. B* **1998**, *102*, 3586 – 3616.
[75] J. C. Phillips, R. Braun, W. Wang, J. Gumbart, E. Tajkhorshid, E. Villa, C. Chipot, R. D. Skeel, L. Kalé, K. Schulten, *J. Comput. Chem.* **2005**, *26*, 1781 – 1802.
[76] J. Phillips, T. Isgro, M. Sotomayor, E. Villa, H. Yu, D. Tanner, Y. Liu, *NAMD tutorial.* **2012**; http://www.ks.uiuc.edu/Training/Tutorials/namd/archive/2012-01-30/namd-tutorial-unix.pdf.
[77] T. Isgro, J. Phillips, M. Sotomayor, E. Villa, H. Yu, D. Tanner, Y. Liu, Z. Wu, D. Hardy, *NAMD tutorial.* **2017**; http://www.ks.uiuc.edu/Training/Tutorials/namd/namd-tutorial-unix.pdf.

Manuscript received: December 5, 2019
Accepted manuscript online: December 30, 2019
Version of record online: February 21, 2020